Tritopic phenanthroline and pyridine tail-tied aza-scorpiands†

Jorge González,[a] José M. Llinares,[b] Raquel Belda,[a] Javier Pitarch,[a] Concepción Soriano,[c] Roberto Tejero,[d] Begoña Verdejo[a] and Enrique García-España*[a]

Received 7th January 2010, Accepted 9th March 2010
First published as an Advance Article on the web 24th March 2010
DOI: 10.1039/b927418a

The synthesis of two new tritopic double-scorpiand receptors in which two equivalent 5-(2-aminoethyl)-2,5,8-triaza[9]-(2,6)-pyridinophane moieties have been linked with 2,6-dimethylpyridine (**L1**) or 2,9-dimethylphenanthroline (**L2**) units is reported for the first time. Their acid–base behaviour and Zn^{2+} coordination chemistry have been studied by pH-metric titrations, molecular dynamic calculations, NMR, UV-Vis and steady-state fluorescence techniques. **L1** and **L2** behave, respectively, as hexaprotic and heptaprotic bases in the experimental conditions used (298.1 ± 0.1 K, 0.15 mol dm^{-3} NaCl, pH range under study 2.0–11.0). These ligands are able to form mono-, bi- and trinuclear Zn^{2+} complexes depending on the Zn^{2+}-receptor molar ratio. Interaction of **L1** and **L2** with pyrophosphate (PPi), tripolyphosphate (TPP) and adenosine 5′-triphosphate (ATP) has been followed by pH-metric titrations, ^{1}H and ^{31}P NMR techniques and molecular dynamic analysis. Finally, formation of mixed complexes Zn^{2+}-**L**-PPi, Zn^{2+}-**L**-TPP and Zn^{2+}-**L**-ATP has been studied for both receptors by potentiometric titrations.

Introduction

Multitopic ligands have received an increased interest in the last years. This interest stems from their potential applications in fields such as molecular recognition, molecular devices, enzyme mimicking and pharmaceutical chemistry.[1–3]

An elegant example of targeting biologically relevant anions has been reported by J.-I. Hong, J. Yoon *et al*. These authors designed a series of binuclear Zn^{2+} complexes that exhibited selective fluorescence response when interacting with pyrophosphate (PPi).[4] PPi is a biological important target because it is the product of the hydrolysis of the nucleotide adenosine-5′-triphosphate (ATP) under cellular conditions and the detection of PPi is being investigated as a real-time DNA sequencing method.[5]

Bicyclam, bicyclen and tricyclen molecules linked by different alkyl and aryl groups display interesting activity as antiviral drugs for the treatment of HIV-1 and HIV-2.[6] Moreover, it has been postulated that metal coordination can reinforce or decrease the activity. In this sense, Kimura *et al.* reported that the Zn^{2+} complex of a tricyclen molecule, in which the tetraazamacrocycles were connected by *para*-phenylene spacers, displayed the highest inhibitory activity for the binding of the regulatory protein Tat to TAR (*trans* activation responsive) element RNA that activates the synthesis of the full length HIV-mRNA.[7]

On the other hand, scorpiand molecules or lariat ethers are analogous terms describing compounds that have a central macrocyclic core with a pendant arm including additional anchoring points.[8–10] These molecules have attracted a lot of interest due to the possibility of regulating the molecular reorganisation of their flexible arm with respect to the macrocyclic core by coordination to metal ions or/and changes in the hydrogen ion concentration of the medium. Therefore, the preparation of new compounds meeting features of double azamacrocycles and scorpiands is an interesting goal due to their recognition capacity, molecular rearrangements and possible biomedical implications.

Here we describe the synthesis, protonation, Zn^{2+} coordination and interaction with PPi, tripolyphosphate (TPP) and ATP of a couple of double-aza-scorpiand receptors in which two 5-(2-aminoethyl)-2,5,8-triaza[9]-(2,6)-pyridinophane moieties have been tied by their tails with 2,6-dimethylpyridine (**L1**) or 2,9-dimethylphenanthroline (**L2**) linkers (Chart 1). We have additionally studied by potentiometry the formation of mixed Zn^{2+}-**L**-PPi, Zn^{2+}-**L**-TPP and Zn^{2+}-**L**-ATP complexes with both receptors.

For means of clarity, with PPi^{4-}, TPP^{5-} and ATP^{4-} we refer to the fully deprotonated anions, while with PPi, TPP and ATP we will be referring either to any of the species present in the multiprotic systems independently of their protonation state or to the whole polyprotic systems.

Results and discussion

Synthesis of the receptors

The synthesis of **L1** and **L2** has been carried out reacting two moles of scorpiand 5-(2-aminoethyl)-2,5,8-triaza[9]-(2,6)-pyridinophane (**L3**) that some of us have previously reported,[10] with one

[a]*Instituto de Ciencia Molecular (ICMOL), Departamento de Química Inorgánica, Universidad de Valencia, Edificio de Institutos de Paterna, Apartado de Correos 22085, 46071, Valencia, Spain. E-mail: enrique.garcia-es@uv.es; Tel: 00 34 963544879*
[b]*Instituto de Ciencia Molecular (ICMOL), Departamento de Química Orgánica, Fundació General de la Universitat de València (FGUV), Edificio de Institutos de Paterna, Apartado de Correos 22085, 46071, Valencia, Spain*
[c]*Departamento de Química Orgánica, Avda. Vicent Andrés Estellés, S/n, 46100 Burjassot, Valencia, Spain*
[d]*Departamento de Química-Física, C/ Dr. Moliner 50, 46100 Burjassot, Valencia, Spain*
† Electronic supplementary information (ESI) available: Additional experimental details and characterization data. See DOI: 10.1039/b927418a

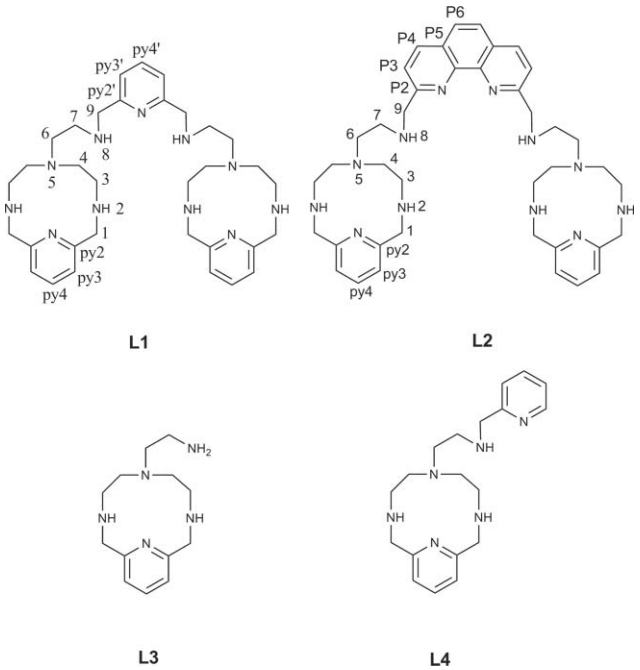

Chart 1

mole of pyridine-2,6-dicarboxaldehyde or 1,10-phenanthroline-2,9-dicarboxaldehyde in dried ethanol, followed by *in situ* reduction with sodium borohydride (see Scheme 1 in the ESI,† and the Experimental section). The compounds were finally precipitated as their hydrochloride salts. Once optimized, this synthetic procedure permits the new receptors **L1** and **L2** to be obtained on a gram scale.

Acid–base studies

To obtain the constants for the interaction of **L1** and **L2** with different guests in aqueous media, the previous determination of the protonation constants of both hosts and guest species in the same experimental conditions is required. Moreover, the knowledge of which are the protonation sites in the receptors at the studied pH values is essential to understand and rationalize their coordinating ability towards either cationic or anionic substrates.

The protonation constants of **L1** and **L2** were obtained by pH-metric titrations carried out at 298.1 K at 0.15 mol dm^{-3} NaCl (see Experimental section for further details). Although chloride anions can interfere in the coordination of metal ions and anions, the scarce solubility of **L2** in perchlorate salts as well as the biological relevance of NaCl led us to use this salt as supporting electrolyte. Since all constants, namely protonation constants of the receptors, formation constants of Zn^{2+} complexes, binding constants with the polyphosphate anions and ATP, and formation constants of mixed complexes have been conducted in the same experimental conditions, the results presented here are self-consistent.

Table 1 gathers the stepwise protonation constants calculated for the protonation of bis-scorpiands **L1–L2**. The distribution diagrams are collected in Fig. S1 of the ESI† and in Fig. 1.

L1 presents in the pH range of study (pH = 2.0–11.0) just six measurable protonation steps (Table 1, Fig. S1†) while **L2** displays an additional seventh protonation step (Fig. 1). The high

Table 1 Logarithms of the stepwise protonation constants for the protonation of **L1** and **L2** determined in 0.15 mol dm^{-3} NaCl at 298.1 K

Reaction[a]	L1	L2
H + L = HL	9.96(2)[b]	10.04(1)
H + HL = H_2L	9.52(2)	9.80(1)
H + H_2L = H_3L	8.51(2)	8.88(1)
H + H_3L = H_4L	7.64(2)	8.15(1)
H + H_4L = H_5L	6.78(3)	6.78(1)
H + H_5L = H_6L	5.94(4)	5.95(1)
H + H_6L = H_7L	—	2.25(2)
Log β[c]	48.34	51.84

[a] Charges omitted for clarity. [b] Values in parentheses are standard deviation in the last significant figure. [c] log $\beta = \Sigma$ log K.

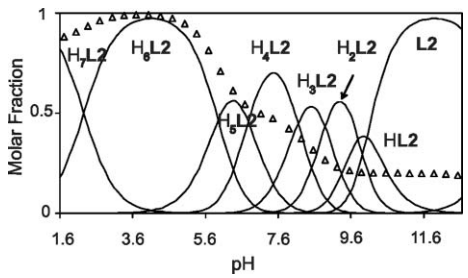

Fig. 1 Molar fraction distribution diagram for the system **L2**-H$^+$ and steady-state fluorescence emission titration curve of **L2** (λ_{exc} = 267 nm) for a 1 × 10^{-5} mol dm^{-3} aqueous solution in 0.15 mol dm^{-3} NaCl at 298.1 ± 0.1 K. (△) monomer emission followed at 376 nm.

six protonation constants observed for both systems make the hexaprotonated species H_6L^{6+} prevail below pH 6 for **L1**, and in a wide 2.5–6.0 pH range for **L2**.[11] While the six first protonation steps of both receptors should occur at the six secondary amino groups present in both receptors, the seventh protonation step of **L2** should involve the connecting phenanthroline group as it has been proved by NMR, UV-Vis and fluorescence emission spectra. The ^{1}H NMR spectra show, below pH 3, clear downfield shifts for signals of the phenanthroline protons labelled as P3, P4 and P6 (for the labelling, see Chart 1), which supports protonation of a phenanthroline nitrogen (see Fig. S2 in the ESI† in which the variations of the ^{1}H NMR signals with the pH are plotted for **L2**).

The UV-Vis titrations of **L2** also show significant changes in the 200–400 nm region in correspondence with the protonation of the phenanthroline ring (Fig. 2). Treatment of the spectrophotometric data with the SPECFIT program[12] allows for deriving a protonation constant of 2.2(1) logarithmic units in good agreement with the constant derived from the potentiometric titrations.

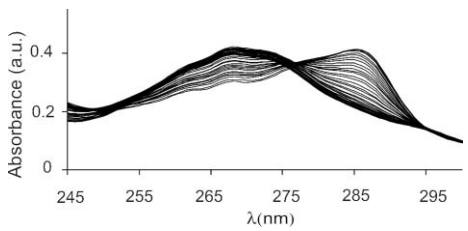

Fig. 2 Spectrophotometric titration of **L2** *vs.* pH recorded in H_2O; T = 298.1 K; l = 1 cm; I = 1.0 mol dm^{-3} (NaCl); [**L2**] = 8.6 × 10^{-5} mol dm^{-3}; (1) pH = 4.5; (2) pH = 1.0.

The variation with the pH of the emission intensity at 376 nm of **L2** shows a bell-shaped curve with the maximum emission corresponding to the pH range where the hexaprotonated species (H_6**L2**$^{6+}$) prevails in solution as can be seen in Fig. 1. Either a protonation or a deprotonation process yields a decrease in fluorescence. The lower emission of the H_7**L2**$^{7+}$ species can be ascribed to the fact that protonation of the phenanthroline can stabilize the poorly emissive nπ* state with respect to the ππ* state, leading to inversion of states and thus to a decrease of the fluorescence emission.[13]

Molecular dynamic calculations[14] suggest that these receptors present two major different families of conformers, (i) a family with more closed conformations that is observed for protonation degrees from 0 to 5 and (ii) a family with more open conformations for higher protonation degrees (Fig. 3). In the closed conformations, intramolecular hydrogen bond networks involving the protonated ammonium groups at each state as hydrogen bond donors and the deprotonated amino groups and the pyridine nitrogen atoms are observed. The composition and number of hydrogen bonds would be changing from one protonation state to another. π–π Stacking between the central pyridine ring and the pyridine ring of one of the macrocycles is also observed in the closed conformation. In the case of **L2**, the molecular dynamics studies indicate that protonation of the phenanthroline ring in the heptaprotonated species leads to an almost completely extended conformation so that electrostatic repulsion between the positive charges are minimized (Fig. 3).

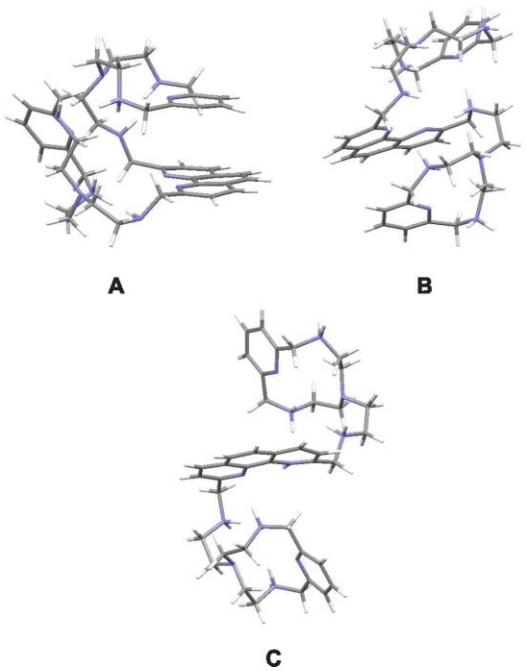

Fig. 3 Minimum energy conformers for receptors H_2**L2** (A), H_6**L2** (B) and H_7**L2** (C).

^{1}H NMR experiments performed at variable pH for both receptors show that all ^{1}H signals experience downfield shifts upon protonation indicating that protons are shared between the different sites (ESI, Fig. S1 and S2†). However, for **L1** the slightly larger downfield shift ($\Delta\delta = 0.87$ ppm, Fig. S1†) observed in the 8.5-10.0 pH range for the singlet signal of pyridyl protons 1 (for the labelling, see Chart 1), suggests that the first two protonations occur to a larger extent at the macrocyclic secondary nitrogen atoms. The next two protons will be preferentially binding the nitrogens of the arms as denoted by the larger downfield shifts of protons labelled as 9 in the 7.0–8.5 pH range. In agreement with the calculations, the variations in the ^{1}H NMR data also suggest the formation of different intramolecular hydrogen bonds between protonated and non-protonated sites and the pyridine in the intermediate protonation sites.

Interaction with metal ions and anions

To check the coordination capabilities of these macrocycles, we have carried out a preliminary study of the interaction of **L1** and **L2** with Zn^{2+}. Moreover, we have studied the interaction of **L1** and **L2** with PPi, TPP and ATP. Finally, we have checked the formation of mixed complexes in the systems Zn^{2+}-**L**-PPi, Zn^{2+}-**L**-TPP and Zn^{2+}-**L**-ATP (**L** = **L1**, **L2**).

Interaction with Zn^{2+}

Potentiometric studies of the binary Zn^{2+}-**L1** and Zn^{2+}-**L2** systems show in both cases formation of mononuclear species of $[ZnH_rL]^{(2+r)+}$ stoichometries with $r = 4$–0, binuclear $[Zn_2H_rL]^{(4+r)+}$ species with $r = 1$, 0, −1 and trinuclear trihydroxylated species for **L1**. In the case of **L2** additional binuclear and trinuclear dihydroxylated species have also been detected. The stability constants for these complexes along with those formed by the precursor scorpiand receptors **L3** and **L4** (Chart 1) are collected in Table 2.[10,15]

As regards the mononuclear complexes, the first aspect that deserves to be commented on is the significant difference in stability between the Zn**L**$^{2+}$ complexes of both receptors, **L1** and **L2**. The stability constant of Zn**L1**$^{2+}$ is higher than those obtained for the Zn^{2+} complexes of the precursor receptors **L3** and comparable to the receptor **L4** (Table 2). Taking into account these values and the crystal structures obtained for the Cu^{2+} complexes of **L3** and **L4**,[10,15] it can be suggested that the binding of the metal in the Zn**L1**$^{2+}$ species is likely involving the four nitrogens of the macrocyclic unit, the secondary nitrogen of the tail and the pyridine nitrogen of the linker (Fig. 4a).

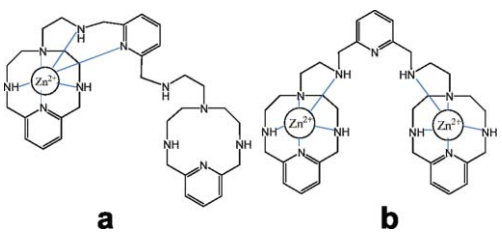

Fig. 4 Possible coordination modes in complexes Zn**L1**$^{2+}$ (a) and Zn_2**L1**$^{4+}$ (b).

In the case of Zn**L2**$^{2+}$, however, the metal ion would be pentacoordinated by the four nitrogen atoms of the macrocycle and the secondary nitrogen atom of the linker.

In both systems, formation of binuclear complexes is observed above pH 4 for Zn^{2+}:**L** 2 : 1 molar ratio (see distribution diagrams in ESI, Fig S3b and Fig. S4b†). The stepwise constants for the formation of the binuclear complexes ($ZnL^{2+} + Zn^{2+} = Zn_2L^{4+}$; log

Table 2 Logarithms of the stability constants for the formation of mononuclear, binuclear and trinuclear complexes of Zn^{2+}:**L1**, **L2**, **L3** and **L4** calculated in 0.15 mol dm^{-3} NaCl at 298.1 ± 0.1 K

Reaction[a]	L1	L2	L3	L4
$ZnH_3L + H = ZnH_4L$	4.24(5)[b]	3.61(1)	—	—
$ZnH_2L + H = ZnH_3L$	4.23(5)	6.28(4)	—	—
$ZnHL + H = ZnH_2L$	7.7(1)	8.48(4)	3.95(4)	—
$ZnL + H = ZnHL$	9.3(1)	10.2(1)	5.23(2)	3.34(2)
$Zn + L = ZnL$	19.8(1)	16.9(1)	17.42(4)	18.97(1)
$ZnL + H_2O = ZnL(OH) + H$	—	—	—	−11.3(3)
$Zn_2L + H = Zn_2HL$	4.83(2)	4.37(1)	—	—
$2Zn + L = Zn_2L$	32.16(2)	33.12(1)	—	—
$ZnL + Zn = Zn_2L$	12.4(1)	16.2(1)	—	—
$Zn_2L + H_2O = Zn_2L(OH) + H$	−10.6(1)	−10.05(2)	—	—
$Zn_2L(OH) + H_2O = Zn_2L(OH)_2 + H$	—	−11.9(1)	—	—
$3Zn + L + 2H_2O = Zn_3L(OH)_2 + 2H$	—	20.46(2)	—	—
$3Zn + L + 3H_2O = Zn_3L(OH)_3 + 3H$	11.5(1)	11.50(3)	—	—

[a] Charges omitted. [b] Values in parenthesis show standard deviation in the last significant figure.

$K = 12.4$ for **L1** and $\log K = 16.2$ for **L2**, (Table 2) show the absence of positive cooperativity in this process. Moreover, the much lower stepwise value obtained for the formation of Zn_2**L1**$^{4+}$ indicates that the binding of the second metal ion will either involve a lower number of nitrogens than in **L2** or will require of a molecular reorganisation of the coordination sphere, implying breaking and bond formation (Fig. 4b).

The distribution diagrams (ESI, Fig. S3 and S4†) show that the nuclearity of the species formed depends very much on the Zn^{2+}-receptor molar ratio. Trinuclear complexes are observed above pH *ca.* 8 for 3 : 1 Zn^{2+} receptor molar ratios for **L1** and pH *ca.* 9 for **L2** (ESI, Fig. S3c and S4c†). Although binuclear complexes have been reported in many systems consisting of two macrocycles linked by different alkyl or aryl bridges, to our knowledge, the number of systems in which trinuclear species has been evidenced is much more scarce.[16,17]

Fig. 5 collects the aromatic zone of the ^{1}H NMR spectra recorded at pD = 10 for the system Zn^{2+}:**L2**, where formation of mono-, bi- and trinuclear species is observed (see ESI, Fig. S3 and S4†). The ^{1}H spectra show significant changes in the pyridine signals when the molar ratio is increased from 1 : 1 to 2 : 1. However, when passing from 2 : 1 to 3 : 1 molar ratios, the largest changes are seen for the phenanthroline signals which shift downfield and broaden considerably, suggesting that the third metal ion is bound at this region of the molecule. The lower number of coordinated nitrogens involved in the coordination sphere of the last metal ion would be favouring the formation of hydroxylated species.

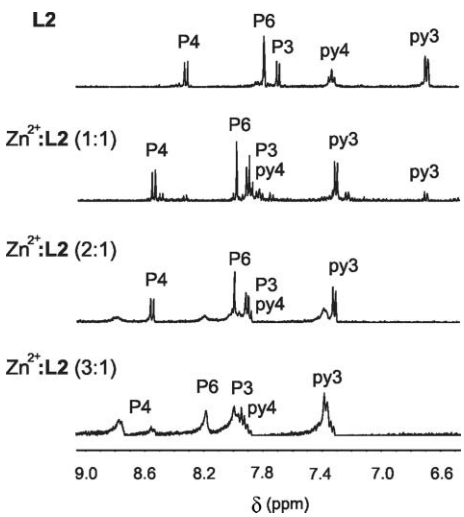

Fig. 5 ^{1}H NMR of Zn^{2+}:**L2** in different molar ratios at pD = 10.0.

Interaction with PPi, TPP and ATP

Interaction of **L1** and **L2** with PPi, TPP and ATP has been followed by potentiometric studies, ^{1}H and ^{31}P NMR spectroscopy, and molecular dynamic analysis. The analysis of the pH-metric titrations with the HYPERQUAD set of programs[18] gave the model and values of the cumulative constants collected in Table S2 of the ESI.†

For all the studied systems only anion-receptor adducts of 1 : 1 stoichiometry have been found. The protonation degrees ranged from 1 to 7 for the systems **L1**-PPi and **L1**-ATP, from 4 to 7 for the system **L1**-TPP, from 1 to 8 for **L2**-PPi and **L2**-ATP, and from 2 to 8 for **L2**-TPP. As shown by the distribution diagrams collected in the ESI (Fig. S5 and Fig. S6†), the adducts prevail in a wide pH range for all the studied systems. The 1 : 1 anion-receptor stoichiometry was also checked by ^{31}P NMR spectroscopy for the systems **L1**-PPi, **L1**-TPP, **L2**-PPi and **L2**-TPP. ^{31}P NMR spectra of D_2O solutions in which increasing amounts of **L1** or **L2** were added either to PPi or to TPP solutions were registered at pD = 5.9 and 7.5 indicating a 1 : 1 anion-receptor stoichiometry (Fig. 6, ESI, Fig. S7, S8 and S9†).

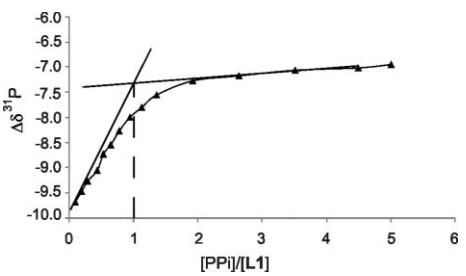

Fig. 6 Plot of $\Delta\delta$ ^{31}P signal of PPi *versus* [PPi]/[**L1**] at pD = 5.9 in D_2O.

Similar results were obtained for ATP, the spectra were recorded in this case at pD = 7.0. The downfield shifts observed for the signals of Pγ and P_β of ATP ($\Delta\delta$ = 3.9 ppm and $\Delta\delta$ = 1.6 ppm, respectively) in the ^{31}P NMR spectra of the system **L1**-ATP confirm the interaction (Fig. 7). As usually happens for these systems, the shift observed for the chemical signal of P_α is more reduced $\Delta\delta = 0.1$ ppm.[19] Interestingly enough, the ^{31}P NMR spectrum of the **L1**-ATP system at pH = 7.0 is coincident with the spectrum of free ATP at pD = 9.0, denoting that the interaction with the polyamine makes ATP more acidic. Moreover, the ^{31}P NMR spectrum at pD = 9.0 of the **L1**-ATP system does not present any difference with the spectrum of free ATP at the same pD. In fact, at this pD, ATP is already in its fully deprotonated ATP^{4-} form and therefore, interaction with the polyammonium receptor cannot produce any change in its protonation degree (Fig. 7). Similar results are obtained for the system **L2**-ATP (ESI, Fig. S10†).

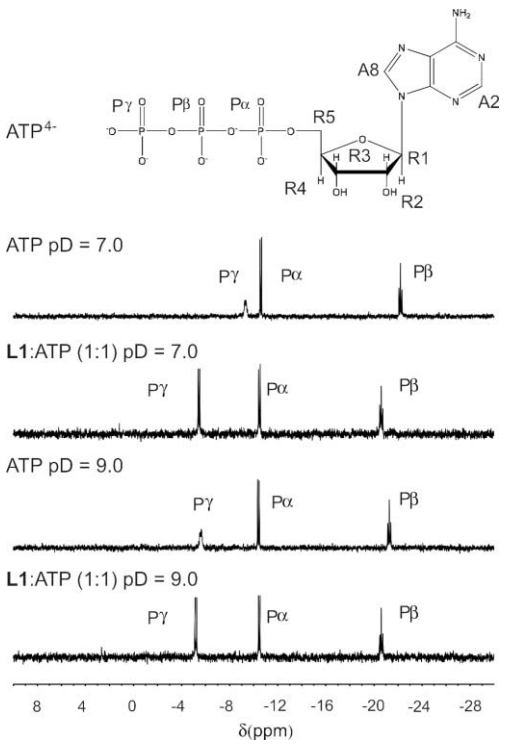

Fig. 7 ^{31}P NMR spectra of **L1** at pD = 7.0 and 9.0 in D_2O.

To translate the values of the cumulative constants into stepwise constants representative of the actual equilibrium occurring in solution, the protonation degrees of substrate and receptors at every equilibrium need to be known and therefore, the basicity constants of substrates and receptors have to be taken into account. By doing this, the stepwise constants collected in Table 3 and 4 have been calculated. These constants clearly show that **L2** interacts stronger with TPP and ATP than **L1**, while PPi displays slightly higher constants with **L1** than with **L2**.

Nevertheless, there is a number of equilibria in which the substrates and receptors have very close basicities and thus, it is difficult to decide if the proton will be in the substrate or in the guest species or even shared between them. The most unambiguous way to compare the relative stabilities of the

Table 3 Logarithms of the stepwise constants for the interaction of **L1** with PPi, TPP and ATP calculated in 0.15 mol dm^{-3} NaCl at 298.1 ± 0.1 K

Reaction[a]	A = PPi^{4-}	A = TPP^{5-}	A = ATP^{4-}
HL + A = HLA	3.12(4)[b]	—	3.63(4)
H_2L + A = H_2LA	3.90(2)	—	3.40(3)
H_3L + A = H_3LA	4.07(5)	—	3.48(4)
H_4L + A = H_4LA	5.03(4)	4.04(4)	4.36(2)
H_3L + HA = H_4LA	4.54(4)	4.13(5)	—
H_5L + A = H_5LA	6.49(3)	5.84(1)	5.54(1)
H_4L + HA = H_5LA	5.13(3)	5.07(1)	5.65(1)
H_5L + HA = H_6LA	5.52(3)	5.09(3)	5.39(1)
H_6L + HA = H_7LA	5.51(3)	3.9(1)	3.84(2)
H_6L + H_2A = H_8LA	5.83(3)	4.5(1)	—

[a] Charges omitted. [b] Values in parenthesis show standard deviation in the last significant figure.

Table 4 Logarithms of the stepwise constants for the interaction of **L2** with PPi, TPP and ATP calculated in 0.15 mol dm^{-3} NaCl at 298.1 ± 0.1 K

Reaction[a]	A = PPi^{4-}	A = TPP^{5-}	A = ATP^{4-}
HL + A = HLA	3.3(1)[b]	—	4.52(3)
H_2L + A = H_2LA	3.58(4)	4.11(1)	4.95(3)
H_3L + A = H_3LA	3.91(6)	4.09(3)	5.34(3)
H_4L + A = H_4LA	4.60(3)	5.05(2)	5.86(2)
H_3L + HA = H_4LA	4.61(4)	5.65(2)	—
H_5L + A = H_5LA	5.98(4)	6.26(2)	6.88(2)
H_4L + HA = H_5LA	4.62(4)	5.49(2)	6.99(2)
H_5L + HA = H_6LA	5.43(3)	6.32(2)	6.88(1)
H_6L + HA = H_7LA	5.88(3)	6.66(2)	7.07(2)
H_6L + H_2A = H_8LA	5.32(4)	5.65(3)	6.64(3)

[a] Charges omitted. [b] Values in parenthesis show standard deviation in the last significant figure.

different systems and to establish selectivity ratios is to use effective constants.[19] The effective constants K_{eff} are calculated at every pH value as the quotient between the overall amount of complexed species and the overall amounts of free receptor and substrate independently of their protonation degree.

$$K_{eff} = \frac{\Sigma[H_{i+j}AL]}{\Sigma[H_iA]\Sigma[H_jL]}$$

Fig. 8 and 9 represent the plot of the logarithms of the effective conditional constant *vs.* pH for the studied systems.

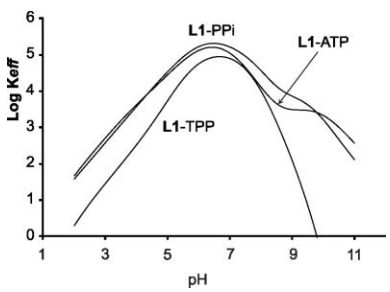

Fig. 8 Plot of the logarithms of the effective constants for the systems **L1**-PPi, **L1**-TPP and **L1**-ATP.

These plots show for **L1** the stability trend PPi ≈ ATP > TPP while for **L2** it would be ATP > TPP >PPi.

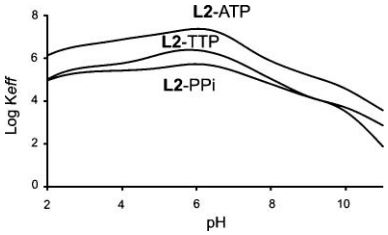

Fig. 9 Plot of the logarithms of the effective constants for the systems **L2**-PPi, **L2**-TPP and **L2**-ATP.

^{1}H NMR spectra coupled with molecular dynamic studies provide interesting structural insights about the interaction of ATP with **L1** and **L2**. The ^{1}H NMR spectra of the systems **L1**-ATP and **L2**-ATP recorded at pH 7.0 and 9.0 show upfield shifts of the aromatic and anomeric signals of ATP (Fig. 10 and 11, and ESI, Fig. S11†) and of selected signals of the aromatic regions of the receptors denoting that stacking occurs in both ligands. For **L2**, the observed shifts are, however, larger than in the case of **L1** in correspondence with the presence of the extended phenanthroline ring.

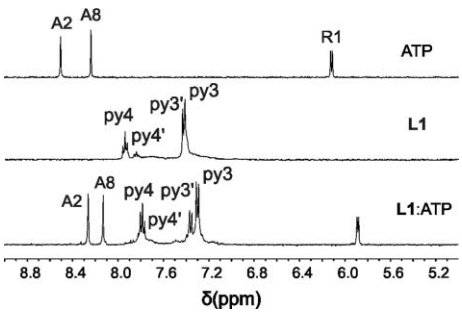

Fig. 10 Upfield region including aromatic and anomeric signals of the ^{1}H NMR spectra of ATP, **L1** and **L1**-ATP recorded in D_2O at pD = 7.0.

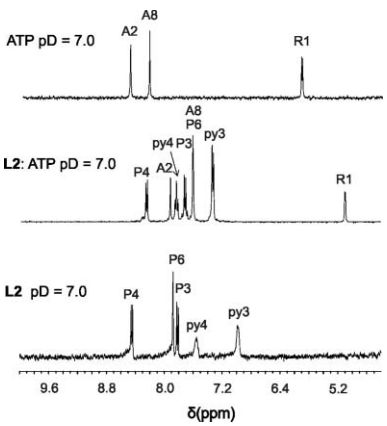

Fig. 11 Upfield region including aromatic and anomeric signals of the ^{1}H NMR spectra of ATP, **L2** and **L2**-ATP recorded in D_2O at pD = 7.0.

Inspection of the shifts of the receptor signals permit some conclusions to be drawn about the structure of the adducts. In the case of **L1**, while the NMR signals of the protons of the macrocyclic pyridine rings shift downfield, those of the protons of the pyridine ring in the central bridge practically do not move, which means that the conformation of the macrocycle is not very much disrupted by the interaction with ATP and the stacking of adenine will occur with the macrocyclic pyridines. This is further confirmed by 1D selective NOE NMR experiments that show intense effects between A2 of adenine and the pyridyl protons of the macrocycles (see ESI, Fig. S12†).

For **L2**, the anomeric and aromatic signals of ATP and the signals from the phenanthroline ring show an important upfield shift, in contrast with the pyridine ring signals that experiences a downfield shift (Fig. 11). Moreover, 1D selective NOE NMR experiments show that irradiation of A2 adenine affects protons of phenanthroline labeled as P3 and P4 (see ESI, Fig. S13†). These shifts indicate that while π–π stacking between adenine and phenanthroline is produced following the formation of the adduct species, the stacking between pyridine and phenanthroline that occurred in the free ligand is being disrupted.

Molecular dynamic calculations for the interaction of H_6**L2**$^{2+}$ and ATP^{4-}, which are the species predominating in solution at neutral pH, show that effectively in the family of minimum energy conformers the adenine ring is stacked with the phenanthroline moiety while no internal stacking is produced in the receptor. The phosphate chain is placed between the macrocyclic rings so that maximum electrostatic interaction is achieved with the positive charges of the receptor (Fig. 12). Fig S14† collects the family of ten minimum energy conformers, which show that this arrangement is conserved in all of them.

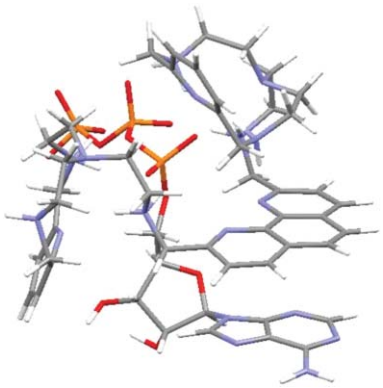

Fig. 12 Minimum energy conformer calculated for the interaction of H_6**L2**$^{6+}$ with ATP.

Formation of mixed complexes

It is well known that metal complexes either with coordinatively unsaturated sites or with ancillary ligand in its coordination sphere can interact with anionic species through coordinative bonds. In our case, although the mononuclear and binuclear complexes seem to be penta or hexacoordinated, the formation of trinuclear species should provide vacant coordination sites for anion interaction. Moreover, even pentacoordinated Zn^{2+} sites might in principle interact with further ligands due to the facility of this $3d^{10}$ metal ion to increase its coordination number to six. Additionally, in the mononuclear complexes the presence of a metal-free macrocyclic unit that can bear protonation may give rise to mixed binding modes. The metal site can provide coordinative bonds while the metal-free macrocycle can interact

Table 5 Logarithms of the stability constants for the formation of the mixed complexes of Zn^{2+} and PPi, TPP and ATP with **L1** calculated in 0.15 mol dm^{-3} NaCl at 298.1 ± 0.1 K

Reaction[a]	A = PPi^{4-}	A = TPP^{5-}	A = ATP^{4-}
$6H + Zn + L + A = ZnH_6LA$	—	—	59.78(4)[b]
$5H + Zn + L + A = ZnH_5LA$	59.1(1)	58.01(8)	55.72(8)
$4H + Zn + L + A = ZnH_4LA$	54.90(4)	54.10(3)	52.61(3)
$3H + Zn + L + A = ZnH_3LA$	48.69(6)	48.30(4)	47.44(4)
$2H + Zn + L + A = ZnH_2LA$	41.13(6)	40.92(4)	40.71(4)
$H + Zn + L + A = ZnHLA$	32.40(8)	32.22(9)	—
$2H + 2Zn + L + A = Zn_2H_2LA$	50.29(4)	50.16(3)	48.23(2)
$H + 2Zn + L + A = Zn_2HLA$	44.58(7)	44.77(4)	43.48(2)
$2Zn + L + A = Zn_2LA$	36.43(4)	36.98(5)	37.09(3)
$H_2O + 2Zn + L + A = Zn_2LA(OH) + H$	—	—	27.50(4)
$3Zn + L + A = Zn_3LA$	—	43.56(2)	41.73(2)
$H_2O + 3Zn + L + A = Zn_3LA(OH) + H$	—	35.16(3)	33.37(3)

[a] Charges omitted. [b] Values in parenthesis show standard deviation in the last significant figure.

Table 6 Logarithms of the stability constants for the formation of the mixed complexes of Zn^{2+} and PPi, TPP and ATP with **L2** calculated in 0.15 mol dm^{-3} NaCl at 298.1 ± 0.1 K

Reaction[a]	A = PPi^{4-}	A = TPP^{5-}	A = ATP^{4-}
$6H + Zn + L + A = ZnH_6LA$	—	64.86(6)	63.73(3)[b]
$5H + Zn + L + A = ZnH_5LA$	62.50(1)	61.70(1)	60.54(1)
$4H + Zn + L + A = ZnH_4LA$	57.20(5)	56.12(8)	55.56(6)
$3H + Zn + L + A = ZnH_3LA$	49.54(5)	49.88((5)	49.15(5)
$2H + Zn + L + A = ZnH_2LA$	42.21(6)	42.34(5)	41.55(5)
$H + Zn + L + A = ZnHLA$	33.45(4)	33.90(5)	32.26(6)
$Zn + L + A = ZnLA$	23.50(7)	24.50(5)	21.74(8)
$2H + 2Zn + L + A = Zn_2H_6LA$	54.52(2)	53.21(3)	52.09(1)
$H + 2Zn + L + A = Zn_2HLA$	49.79(3)	47.79(4)	46.19(2)
$2Zn + L + A = Zn_2LA$	41.59(5)	40.00(6)	36.31(6)
$H_2O + 2Zn + L + A = Zn_2LA(OH) + H$	31.45(5)	29.97(6)	27.50(4)
$2H + 3Zn + L + A = Zn_3H_2LA$	—	—	55.66(3)
$H + 3Zn + L + A = Zn_3HLA$	53.99(4)	52.71(4)	50.99(4)
$3Zn + L + A = Zn_3LA$	49.27(4)	47.76(4)	42.8(1)
$H_2O + 3Zn + L + A = Zn_3LA(OH) + H$	41.11(4)	39.24(7)	34.82(4)
$2H_2O + 3Zn + L + A = Zn_3LA(OH)_2 + 2H$	31.50(6)	29.48(6)	25.3(1)

[a] Charges omitted. [b] Values in parenthesis show standard deviation in the last significant figure.

through hydrogen bonds and when protonated also through charge-charge interactions with the anion.

We have studied the interaction of the Zn^{2+} complexes of **L1** and **L2** with PPi, TPP and ATP. For TPP, complexes of stoichiometries $[ZnH_rLTPP]^{(r-3)+}$ (**L1**, r = 1–5; **L2**, r = 0–6), $[Zn_2H_rLTPP]^{(r+1)+}$ (**L1**, r = 0–2; **L2**, r = −1–2) and $[Zn_3LTPP]^{(2+r)+}$ (**L1**, r = −1–0; **L2**, r = −2–1), and for ATP the complexes of stoichiometries $[ZnH_rLATP]^{(r-2)+}$ (**L1**, r = 2–6; **L2**, r = 0–6), $[Zn_2H_rLATP]^{r+}$ (**L1**, r = −1–2; **L2**, r = −1–2) and $[Zn_3L1ATP]^{(2+r)+}$ (**L1**, r = −1–0; **L2**, r = −2–2) have been detected. In the case of PPi complexes of stoichiometries $[ZnH_rLPPi]^{(r-2)+}$ (**L1**, r = 1–5; **L2**, r = 0–5), $[Zn_2H_rLPPi]^{r+}$ (**L1**, r = 0–2; **L2**, r = −1–2) while for **L2** complexes of $[Zn_3H_rL2PPi]^{(r+2)+}$ (r = −2–1) were also detected. The occurrence of precipitation when working in Zn^{2+} : **L1** : PPi 3 : 1 : 1 molar ratios made the data not amenable to analysis.

The cumulative binding constants are presented in Table 5 and 6. Fig. 13 and 14 collect, respectively, the distribution diagram for the systems Zn^{2+}-**L1**-ATP and Zn^{2+}-**L2**-ATP for molar ratios 1 : 1 : 1, 2 : 1 : 1 and 3 : 1 : 1.

The distribution diagrams in Fig. 13 and 14, and the distribution diagrams for the other studied systems, which are collected in the ESI (Fig. S15–S18†) show that the mixed complexes predominate throughout a wide pH range. Binary anion-receptor complexes are only observed at acidic pH values where the zinc complexes are not yet formed. Also disruption of the ternary complexes is observed for Zn^{2+} : **L** 3 : 1 molar ratio at basic pH values, where the hydroxo anions compete with ATP for binding to the anion.

Decomposition of the cumulative constants into representative stepwise constants is rather cumbersome due to the multiple overlapped equilibria occurring in solution. However, one way of comparing the efficiency of the Zn^{2+}-**L1** and Zn^{2+}-**L2** to bind ATP is to calculate the distribution diagrams for the Zn^{2+}-**L1**-**L2**-ATP system in appropriate molar ratios and represent the amount of ATP coordinated to Zn^{2+}-**L1** or to Zn^{2+}-**L2** against the pH. As an example, Fig. 15, which collects such representations for the Zn^{2+}-**L1**-**L2**-ATP system for molar ratios 2 : 1 : 1 : 1, 4 : 1 : 1 : 1 and 6 : 1 : 1, puts into evidence that, in general and similarly to what happened in the binary systems, ATP is bound preferentially by

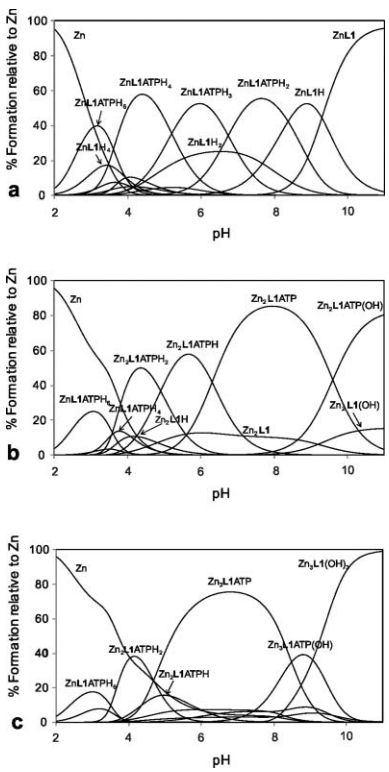

Fig. 13 Distribution diagrams of the species for the Zn^{2+}:**L1**:ATP systems as a function of pH in aqueous solution in 0.15 mol dm^{-3} at 298.1 K; [**L1**] = 1×10^{-3} mol dm^{-3}, [ATP] = 1×10^{-3} mol dm^{-3}. (a) $[Zn^{+2}] = 1 \times 10^{-3}$ mol dm^{-3}, (b) $[Zn^{+2}] = 2 \times 10^{-3}$ mol dm^{-3} and (c) $[Zn^{+2}] = 3 \times 10^{-3}$ mol dm^{-3}.

the Zn**L2** complexes. Similar conclusions can be derived for the other two anions (ESI, Fig. S19–S20†).

A question that remains open is whether the introduction of the metal ions leads to greater amounts of complexation of the anions with respect to the systems in the absence of metal ions.

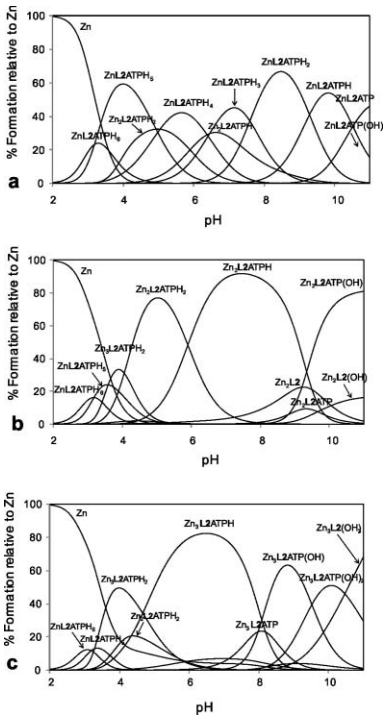

Fig. 14 Distribution diagrams of the species for the Zn^{2+}:**L2**:ATP systems as a function of pH in aqueous solution in 0.15 mol dm^{-3} at 298.1 K; [**L2**] = 1×10^{-3} mol dm^{-3}, [ATP] = 1×10^{-3} mol dm^{-3}. (a) $[Zn^{+2}] = 1 \times 10^{-3}$ mol dm^{-3}, (b) $[Zn^{+2}] = 2 \times 10^{-3}$ mol dm^{-3} and (c) $[Zn^{+2}] = 3 \times 10^{-3}$ mol dm^{-3}.

To address this point, we have plotted the amounts of complexed anionic substrates either in the absence of metal or in the presence of one, two and three equivalents of Zn^{2+} (Fig. 16 and ESI, S21–22†). Fig. 16 shows this representation for ATP. It can be seen that although the addition of the metal ion favours the complexation of the anion at basic pH values, the percentages of complexed anions are quite close in the remaining pH window. As above mentioned, only at the acidic pH values in which formation of Zn^{2+} complexes does not occur, the binary species anion-**L** predominate.

These results support again the high coordination numbers inferred from the speciation studies for the Zn^{2+} complexes. In these complexes, the nitrogen atoms will either fully or almost fully occupy the coordination spheres and there is no available room for new ligands to get close to the metal and therefore, the interaction with the anion should mainly be of charge to charge nature. It is only for the trinuclear complexes where significant differences in the amounts of complexed anionic species are found for the free and complexed systems. This can be ascribed to the fact that there are not enough nitrogen atoms to saturate the coordination sphere of the third metal ion. Nevertheless, as the metal complex almost quantitatively complex the anions in the form of mixed species, this should represent a new binding mode that can be of relevance in various respects, one of them the likely interaction of these systems with nucleic acids, which we are currently exploring.

Conclusions

The synthesis of two new tail-tied aza macrocycles in which two pyridinophane scorpiand equivalent units have been covalently connected through 2,6-dimethylpyridine or 2,9-dimethylphenanthroline linkages is achieved through a straight through synthetic procedure that permits the compounds to be obtained on a gram scale. The number of nitrogen atoms is sufficient to provide penta- or even hexacoordinated mononuclear and binuclear complexes. Both ligands interact strongly with PPi, TPP and ATP as proved by pH-metric and NMR techniques.

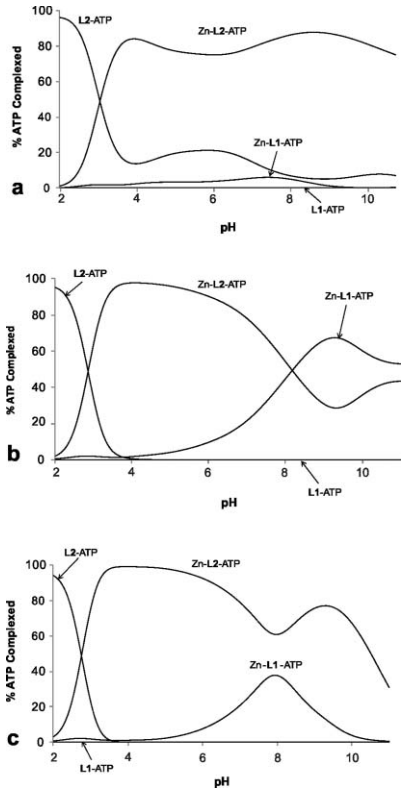

Fig. 15 Representation of the percentages of complexed ATP to **L1**, **L2** and to Zn^{2+}-**L1** and to Zn^{2+}-**L2** *versus* pH calculated from distribution diagrams of the species for the Zn^{2+}:**L1**:**L2**:ATP calculated for concentrations dm^{-3} at 298.1 K; [**L1**] = [**L2**] [ATP] = 1×10^{-3} mol dm^{-3}. (a) $[Zn^{+2}] = 2 \times 10^{-3}$ mol dm^{-3}, (b) $[Zn^{+2}] = 4 \times 10^{-3}$ mol dm^{-3} and (c) $[Zn^{+2}] = 6 \times 10^{-3}$ mol dm^{-3}.

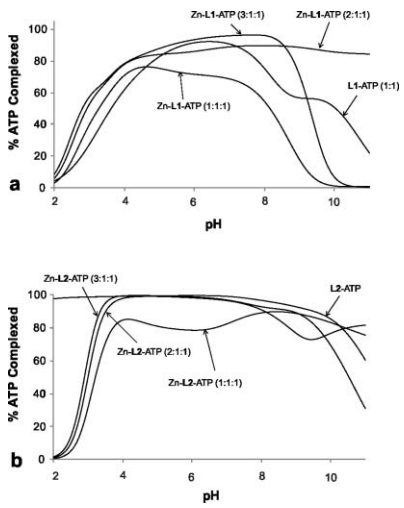

Fig. 16 Overall amounts of complexed anions in the binary and ternary systems of ATP for (a) **L1** and (b) **L2**.

Stacking interactions are clearly evidenced for the interaction of ATP with **L2** containing condensed aromatic rings. Although formation of mixed complexes Zn^{2+}-**L**-anion occurs at a large extent, the amounts of complexed anion by the Zn^{2+}-**L** complexes are only clearly higher than those attained by the free ligand at basic pHs. The versatility and different binding modes for anionic species displayed by these tail-tied receptors make them appealing candidates for interaction and activation of nucleic acids. We are currently exploring this point.

Experimental section

Synthesis of L1

5-(2-Aminoethyl)-2,5,8-triaza[12]-2,6-pyridinophane[10] (1.04 g, 4.16 mmol) and 2,6-pyridinedicarboxaldehyde (0.28 g, 2.08 mmol) were dissolved in 40 mL anhydrous ethanol and the mixture was stirred for 2 h at room temperature. $NaBH_4$ (0.78 g, 20.70 mmol) was then added and the resulting solution stirred for 2 h at room temperature. The ethanol was removed under reduced pressure. The resulting residue was treated with H_2O (10 mL) and extracted with CH_2Cl_2 (3 × 20 mL). The organic phase was removed at reduced pressure, and the resulting residue was dissolved in ethanol and precipitated as hydrochloride salt of **L1** in 63% yield (see Scheme 1 in the ESI†). mp: 223–225 °C. ^{1}H NMR (300 MHz, D_2O): δ (ppm) = 7.64 (t, 2H, J = 8 Hz), 7.63 (t, 1H, J = 8 Hz), 7.18 (d, 2H, J = 8 Hz), 7.13 (d, 4H, J = 8 Hz), 4.32 (s, 8H), 4.18 (s, 4H), 3.11-3.16 (m, 4H), 2.85-2.96 (m, 12H), 2.62-2.65 (m, 8H). ^{13}C NMR (75.43 MHz, D_2O): δ (ppm) = 140.1, 139.7, 123.5, 122.5, 51.4, 51.2, 50.9, 49.8, 46.3, 43.5.

Calc for $C_{33}H_{51}N_{11}\cdot 6HCl\,4H_2O$: C, 44.4; H, 7.3; N, 17.3. Found: C, 44.6; H, 7.7; N, 16.5. *MS* (*FAB*) *m*/*z* 601 $[M]^+$

Synthesis of L2

5-(2-Aminoethyl)-2,5,8-triaza[12]-2,6-pyridinophane[10] (1.04 g, 4.16 mmol) and 1,10-phenanthroline-2,9-dicarboxaldehyde[20] (0.49 g, 2.08 mmol) were dissolved in 40 mL anhydrous ethanol and the mixture was stirred for 2 h at room temperature. $NaBH_4$ (0.78 g, 20.70 mmol) was then added and the resulting solution stirred for 2 h at room temperature. The ethanol was removed under reduced pressure. The resulting residue was treated with H_2O (10 mL) and extracted with CH_2Cl_2 (3 × 20 mL). The organic phase was removed at reduced pressure and the resulting residue was dissolved in ethanol and precipitated as hydrochloride salt of **L2** in 50% yield. mp: decomp. 345 °C. ^{1}H NMR (300 MHz, D_2O): δ (ppm) = 8.73 (d, J = 8 Hz, 2H), 8.12 (s, 2H), 8.03 (d, J = 8 Hz, 2H), 7.95 (t, J = 7 Hz, 2H), 7.44 (d, J = 7 Hz, 4H), 4.87 (s, 4H), 4.62 (s, 8H), 3.60-3.53 (m, 4H), 3.31-3.20 (m, 12H), 3.00-2.90 (m, 8H). ^{13}C NMR (75.43 MHz, D_2O): δ (ppm) = 150.6, 149.0, 141.7, 141.3, 139.9, 129.8, 127.8, 124.6, 122.3, 51.4, 51.2, 50.8, 49.6, 46.1, 43.8.

Calc for $C_{40}H_{54}N_{12}\cdot 6HCl$: C, 52.5; H, 5.9; N, 18.4. Found: C, 52.8; H, 8.0; N, 18.2. *MS* (*FAB*) *m*/*z* 704 $[M+H]^+$

EMF measurements

The potentiometric titrations were carried out at 298.1 ± 0.1 K using NaCl 0.15 M as supporting electrolyte. The experimental procedure (burette, potentiometer, cell, stirrer, microcomputer, *etc.*) has been fully described elsewhere.[21] The acquisition of the EMF data was performed with the computer program PASAT.[22] The reference electrode was an Ag/AgCl electrode in saturated KCl solution. The glass electrode was calibrated as a hydrogen ion concentration probe by titration of previously standardized amounts of HCl with CO_2-free NaOH solutions and the equivalent point determined by the Gran's method,[23] which gives the standard potential, $E°'$, and the ionic product of water (pKw = 13.73(1)).

The computer program HYPERQUAD was used to calculate the protonation and stability constants.[18] The HYSS[24] program was used to obtain the distribution diagrams The pH range investigated was 2.5-11.0. In the binary Zn^{2+}-**L1** and Zn^{2+}-**L2** systems, the concentration of Zn^{2+} and of the ligands ranged from 1×10^{-3} to 5×10^{-3} mol dm^{-3} with Zn^{2+} : L molar ratios varying from 2 : 1 to 1 : 2. In the binary PPi-**L**, TPP-**L** and ATP-**L** systems concentrations of the anion and of the receptors go from 1×10^{-3} mol dm^{-3} to 5×10^{-3} mol dm^{-3}. The protonation constants for ATP, PPi and TPP were either taken from ref. 19 (ATP) or redetermined in our experimental conditions.

For the ternary systems, aqueous solutions at acidic pH containing Zn^{2+} : **L** : anion in 1 : 1 : 1, 2 : 1 : 1 or 3 : 1 : 1 molar ratios were titrated with NaOH solutions. The formation constants of Zn^{2+}-PPi, Zn^{2+}-TPP and Zn^{2+}-ATP were taken from the literature[25] or re-determined under our experimental conditions (PPi, log β_{ZnL} = 9.52(1); TPP, log β_{ZnL} = 6.68(1), log β_{ZnHL} = 11.78(2), log $\beta_{ZnL(OH)}$ = −2.21(2). The titration curves for each system (at least two titrations, *ca.* 200 experimental) were treated either as a single set or as separated curves without significant variations in the values of the stability constants.

When more than one model could fit the experimental data, the most reliable chemical model was chosen by performing F tests at the 0.05 confidence level.[26,27]

NMR measurements

The ^{1}H and ^{13}C spectra were recorded on a Bruker 300 DRX spectrometer at 300 MHz for ^{1}H and 75.43 MHz for ^{13}C. The NMR experiments involving ^{31}P were recorded on a Varian Unity 300 spectrometer equipped with a switchable probe. The chemical shifts were recorded in ppm. All spectra were recorded at room temperature and the concentration of **L1**·6HCl, **L2**·6HCl, PPi, TPP and ATP was 2 mM in D_2O and the $[Zn^{2+}]$ was kept between 2-6 mM. The pD was adjusted with a concentrated solution of DCl or NaOD in D_2O. 1D-NMR experiments were recorded in a Bruker AV 500.

Molecular dynamics simulations

Molecular dynamics simulations were carried out using AMBER8 and GAFF potentials at 325 K.[14] The process comprised a convenient heating stage (in several steps until a final temperature of 325 K is reached) after which the simulation was done. The heating stage comprised 6 steps along which the temperature was slowly increased for a period of 30 picoseconds plus 2 steps, of 20 picosecond each, at the end until the target temperature was reached, namely 325 K. Then the system was ready for a production stage of 77 nanoseconds along which energies and data were saved every 500 steps (each step 0.2 femtoseconds). Minimum energy conformers were extracted from the trajectories. Files with

trajectories in AMBER8 format and GAFF potentials at 325 K are available on request.[14]

Acknowledgements

Financial support from Ministerio de Ciencia e Innovación (CTQ2006-15672-CO5-01). J.G. wants to thank Ministerio de Educación y Ciencia (Spain) for his FPU fellowship. One of us (J. P.) wants to thank Generalitat Valenciana for a Geronimo Forteza formation contract.

Notes and references

1 (*a*) J. M. Lehn, *Supramolecular Chemistry. Concepts and Perspectives*, VCH, Weinheim, 1995; (*b*) H. J. Schneider, *Principles and Methods in Supramolecular Chemistry*, John Wiley & Sons, Chichester, UK, 2000; (*c*) *Supramolecular Chemistry of Anions*, ed. A. Bianchi, K. Bowman-James and E. García-España, John Wiley & Sons, Chichester, UK, 1997; (*d*) J. L. Sessler, P. A. Gale and W. S. Cho, *Anion Receptor Chemistry*, RSC Publishing, Cambridge, UK, 2006; (*e*) C. Caltagirone and P. A. Gale, *Chem. Soc. Rev.*, 2009, **38**, 520; (*f*) J. W. Steed, *Chem. Soc. Rev.*, 2009, **38**, 506; (*g*) S. Kubik, C. Reyheller and S. Stuwe, *J. Inclusion Phenom. Macrocyclic Chem.*, 2005, **52**, 137; (*h*) H. J. Schneider and A. K. Yatsimirsky, *Chem. Soc. Rev.*, 2008, **37**, 263.

2 (*a*) C. Bazzicalupi, A. Bencini, A. Bianchi, A. Danesi, C. Giorgi, C. Lodeiro, F. Pina, S. Santarelli and B. Valtancoli, *Chem. Commun.*, 2005, 2630; (*b*) Q. X. Xiang, J. Zhang, P. Y. Liu, C. Q. Xia, Z. Y. Zhou, R. G. Xie and X. Q. Yu, *J. Inorg. Biochem.*, 2005, **99**, 1661; (*c*) E. García-España, P. Gaviña, J. Latorre, C. Soriano and B. Verdejo, *J. Am. Chem. Soc.*, 2004, **126**, 5082.

3 (*a*) S. K. Kim, D. H. Lee, J.-I. Hong and J. Yoon, *Acc. Chem. Res.*, 2009, **42**, 23; (*b*) S. Develay, R. Tripier, M. Le Baccon, V. Patinec, G. Serratrice and H. Handel, *Dalton Trans.*, 2006, 3418; (*c*) S. Aoki, H. Kawatani, T. Goto, E. Kimura and M. Shiro, *J. Am. Chem. Soc.*, 2001, **123**, 1123; (*d*) M. T. Albelda, J. C. Frias, E. García-España and S. V. Luis, *Org. Biomol. Chem.*, 2004, **2**, 816.

4 (*a*) A. S. Delépine, R. Tripier and H. Handel, *Org. Biomol. Chem.*, 2008, **6**, 1743; (*b*) D. H. Lee, J. H. Im, S. U. Son, Y. K. Chung and J.-I. Hong, *J. Am. Chem. Soc.*, 2003, **125**, 7752; (*c*) D. H. Lee, S. Y. Kim and J.-I. Hong, *Angew. Chem., Int. Ed.*, 2004, **43**, 4777; (*d*) H. N. Lee, Z. Xu, S. K. Kim, K. M. Swamy, Y. Kim, S.-J. Kim and J. Yoon, *J. Am. Chem. Soc.*, 2007, **129**, 3828.

5 (*a*) M. Ronaghi, S. Karamohamed, B. Pettersson, M. Uhlén and P. Nyrén, *Anal. Biochem.*, 1996, **242**, 84; (*b*) S. Xu, M. He, H. Yu, X. Cai, X. Tan, B. Lu and B. Shu, *Anal. Biochem.*, 2001, **299**, 188.

6 (*a*) G. J. Bridger, R. T. Skerlj, S. Padmanabhan, S. A. Martelluci, G. W. Henson, M. J. Abrams, H. C. Joao, M. Witvrouw, K. de Vreese, R. Pauwels and E. de Clercq, *J. Med. Chem.*, 1996, **39**(1), 109; (*b*) Z. Guo and P. J. Sadler, *Adv. Inorg. Chem.*, 2000, **48**, 183.

7 E. Kikuta, S. Aoki and E. Kimura, *J. Am. Chem. Soc.*, 2001, **123**, 7911.

8 (*a*) T. J. Lotz and T. A. Kaden, *J. Chem. Soc., Chem. Commun.*, 1977, 1; (*b*) V. Amendola, L. Fabbrizzi, M. Lichelli, C. Mangano, P. Pallavicini, L. Parodi and A. Poggi, A., *Coord. Chem. Rev.*, 1999, **190–192**, 649; (*c*) G. W. Gokel, *Chem. Soc. Rev.*, 1992, **21**, 39; (*d*) G. W. Gokel, L. J. Barbour, S. L. De Wall and E. S. Meadows, *Coord. Chem. Rev.*, 2001, **222**, 127.

9 (*a*) V. Amendola, D. Esteban-Gómez, L. Fabbrizzi, M. Licchelli, E. Monzani and F. Sancenón, *Inorg. Chem.*, 2005, **44**, 8690; (*b*) L. Fabbrizzi, M. Licchelli, P. Pallavicini and L. Parodi, *Angew. Chem., Int. Ed.*, 1998, **37**, 800; (*c*) S. Aoki, D. Kagata, M. Shiro, K. Takeda and E. Kimura, *J. Am. Chem. Soc.*, 2004, **126**, 13377; (*d*) S. Aoki, K. Iwaida, N. Hanamoto, M. Shiro and E. Kimura, *J. Am. Chem. Soc.*, 2002, **124**, 5256.

10 B. Verdejo, A. Ferrer, S. Blasco, C. E. Castillo, J. González, J. Latorre, M. A. Máñez, M. G. Basallote, C. Soriano and E. García-España, *Inorg. Chem.*, 2007, **46**, 5707.

11 A. Bencini, A. Bianchi, E. García-España, M. Micheloni and J. A. Ramírez, *Coord. Chem. Rev.*, 1999, **188**, 97.

12 (*a*) SPECFIT, *A Program for Global Least Square Fitting of Equilibrium and Kinetic Systems using Factor Analysis and Marquardt Minimization*, Version 1-26; 4 Spectrum Software Associates, Chapel Hill, NC, 1996; (*b*) H. Gampp, M. Maeder, C. J. Meyer and A. D. Zuberbuhler, *Talanta*, 1985, **32**, 95; (*c*) H. Gampp, M. Maeder, C. J. Meyer and A. D. Zuberbuhler, *Talanta*, 1985, **32**, 257; (*d*) H. Gampp, M. Maeder, C. J. Meyer and A. D. Zuberbuhler, *Talanta*, 1986, **33**, 943.

13 (*a*) C. Bazzicalupi, A. Bencini, A. Bianchi, C. Giorgi, V. Fusi, B. Valtancoli, M. A. Bernardo and F. Pina, *Inorg. Chem.*, 1999, **38**, 3806; (*b*) A. Bencini, M. A. Bernardo, E. García-España, C. Giorgi, S. V. Luis, F. Pina and B. Valtancoli, *Advances in Supramolecular Chemistry*, ed. G. Gokel, 2002, **8**, 79.

14 Molecular dynamics calculations were performed using AMBER8: D. A. Case, T. A. Darden, T. E. Cheatham III, C. L. Simmerling, J. Wang, R. E. Duke, R. Luo, K. M. Merz, B. Wang, D. A. Pearlman, M. Crowley, S. Brozell, V. Tsui, H. Gohlke, J. Mongan, V. Hornak, G. Cui, P. Beroza, C. Schafmeister, J. W. Caldwell, W. S. Ross and P. A. Kollman, *AMBER 8*, 2004, University of California, San Francisco, and AFF potentials; J. Wang, R. M. Wolf, J. W. Caldwell, P. A. Kolman and D. A. Case, *J. Comput. Chem.*, 2004, **25**, 1157 at 325 K.

15 **L4** has been obtained by reacting **L3** with 2-pyridinecarbaldehyde. ^{1}H NMR (D_2O, 300 MHz): δ_H 2.93 (t, $J = 5$ Hz, 4H), 3.13 (t, $J = 8$ Hz, 2H), 3.28 (t, $J = 5$ Hz, 4H), 3.45 (t, $J = 8$ Hz, 2H), 4.57 (s, 2H), 4.64 (s, 4H), 7.45 (d, $J = 8$ Hz, 2H), 7.75 (ddd, $J_1 = J_2 = 8$ Hz, $J_3 = 1$ Hz, 1H), 7.83 (d, $J = 8$ Hz, 1H), 7.96 (t, $J = 8.0$ Hz, 1H), 8.25 (ddd, $J_1 = J_2 = 8$ Hz, $J_2 = 2$ Hz, 1H), 8.72 (dd, $J_1 = 5$ Hz, $J_2 = 1$ Hz, 1H).^{13}C NMR (D_2O, 75.43 MHz): δ_C 43.9, 46.2, 49.8, 50.0, 50.8, 51.2, 122.5, 126.5, 126.6, 140.1, 143.3, 146.8, 147.6, 149.2. Anal Calcd. For $C_{19}H_{28}N_6 \cdot 3HCl$:C, 50.68; H, 6.94; N, 18.75. Found: C, 50.3, H, 7.1; N 18.5. S. Blasco, B. Verdejo, M. P. Clares, C. E. Castilllo, A. Algarra, J. Latorre, M. A. Mañez, M. García-Basallote, C. Soriano and E. García-España, work in preparation.

16 (*a*) E. Kimura, M. Kikuchi, H. Kitamura and T. Koike, *Chem.–Eur. J.*, 1999, **5**, 3113; (*b*) G. Ambrosi, M. Formica, V. Fusi, L. Giorgi, E. Macedi, M. Micheloni, P. Paoli and P. Rossi, *Inorg. Chem.*, 2009, **48**, 10424.

17 (*a*) M. Arca, A. Bencini, E. Berni, C. Caltagirone, F. A. Devillanova, F. Isaia, A. Garau, C. Giorgi, V. Lippolis, A. Perra, L. Tei and B. Valtancoli, *Inorg. Chem.*, 2003, **42**, 6929; (*b*) A. Bencini, E. Berni, A. Bianchi, C. Giorgi, B. Valtanacoli, D. K. Chand and H. J. Schneider, *Dalton Trans.*, 2003, 793; (*c*) A. Bencini, S. Biagini, C. Giorgi, H. Handel, M. L. Baccon, P. Mariani, P. Paoletti, P. Paoli, P. Rossi, R. Tripier and B. Valtancoli, *Eur. J. Org. Chem.*, 2009, 5610.

18 P. Gans, A. Sabatini and A. Vacca, *Talanta*, 1996, **43**, 1739.

19 (*a*) M. T. Albelda, J. Aguilar, S. Alves, R. Aucejo, P. Diaz, C. Lodeiro, J. C. Lima, E. García-España, F. Pina and C. Soriano, *Helv. Chim. Acta*, 2003, **86**, 3118; (*b*) A. Bencini, A. Bianchi, E. García-España, E. C. Scott, L. Morales, B. Wang, T. Deffo, F. Takusagawa, M. P. Mertes, K. B. Mertes and P. Paoletti, *Bioorg. Chem.*, 1992, **20**, 8.

20 C. J. Chandler, L. W. Deady and J. A. Reiss, *J. Heterocycl. Chem.*, 1981, **18**, 599.

21 E. García-España, M. J. Ballester, F. Lloret, J. M. Moratal, J. Faus and A. Bianchi, *J. Chem. Soc., Dalton Trans.*, 1988, 101.

22 M. Fontanelli and M. Micheloni, *Proceedings of the I Spanish-Italian Congress on Thermodinamics of Metal Complexes*, Peñíscola, Castellón, 1990. Program for the automatic control of the microburette and the acquisition of the electromotive force readings.

23 (*a*) G. Gran, *Analyst*, 1952, **77**, 661; (*b*) F. J. Rossotti and H. Rossotti, *J. Chem. Educ.*, 1965, **42**, 375.

24 P. Gans, *Programs to determinethe distribution of Species in multiequilibria systems from the stability constants and mass balance equations.*.

25 R. M. Smith and A. E. Martell, *NIST Stability Constants Database, version 4.0*, National Institute of Standards and Technology, Washington D.C., 1997.

26 W. C. Hamilton, *Statistics in Physical chemistry*, The Ronald Press Co., New York, 1964.

27 L. Bologni, A. Sabatini and A. Vacca, *Inorg. Chim. Acta*, 1983, **69**, 71.

